Two-dimensional analysis of tandem/staggered airfoils using computational fluid dynamics

Z. Husain, M. Z. Abdullah (corresponding author) and T. C. Yap
School of Mechanical Engineering, University Sains Malaysia, Penang, Malaysia
E-mail: mezul@eng.usm.my

Abstract The two-dimensional analysis, using computational fluid dynamics (CFD), of tandem/staggered arranged airfoils of the canard and wing of an Eagle 150 aircraft and also the aerodynamic tests conducted in an open-circuit wind tunnel are presented in the paper. The wind tunnel tests were carried out at a speed of 38 m/s in a test section of size 300 mm (width), 300 mm (height) and 600 mm (length), at Reynolds number 2.25×10^5. The tests were carried out with tandem and staggered placement of the airfoils in order to determine the optimum position of the wing with respect to the canard and also to determine the lift coefficient at various angles of attack. The CFD code FLUENT 5 was used to investigate the aerodynamic performance of a two-dimensional model to validate the wind tunnel results. The flow interaction was studied in the tandem and staggered arrangements in the wind tunnel as well as by the computational method. The k-ε turbulence model gave exceptionally good results.

Keywords canard/wing arrangement; lift coefficient; drag coefficient; boundary layer thickness; k-ε turbulence model

Introduction

Theoretical research conducted by McGee and Kroo [1] has suggested that a tandem wing configuration can be optimized better than conventional configurations under all flight conditions of an aircraft. Proper utilization of a canard, however, requires an understanding of the inflow of the canard and flow behavior over the main wing. Two-dimensional analysis has been a subject of research for some decades because of special interest in the structure and dynamics of airflow wakes as a function of the Reynolds number. Calarese [2] studied close-coupled canard–wing vortex interactions. The tests were performed at low Mach numbers and various angles of attack. Three configurations were studied: (1) coplanar, (2) canard placed higher than the wing, and (3) without canard. The results showed that the flow at the leading edge of sweptback wings at a moderate or high angle of attack separates and produces vortex sheets that roll up into vortices on the wing's upper surface. Interference changes the turbulence characteristics and the trajectories of the vortices. The influence of canards on wing aerodynamics can often result in increased lift and decreased trim drag.

Tu [3] investigated canard–wing interactions for high, middle and low canard positions. The computational results showed favorable results for high and middle canard positions. Tu concluded that proper positioning of canards is essential to optimize aerodynamic performance as well as stability and control characteristics. A study of tandem-airfoil interactions in different regimes using computational

methods has been done by Fanjoy and Dorney [4]. A two-dimensional tandem airfoil geometry comprising two NACA airfoils was tested at subsonic and sonic speeds. A symmetrical configuration was selected and experiments were performed in which the distance between the mid-chords of each airfoil was varied. The results showed that, at positive angles of attack, the lift/drag ratio of the lead airfoil is increased while the trailing airfoil experiences less lift and drag, due to a reduced local angle of attack. The phenomena became more prevalent when the stagger distance increased. The paper did not consider determination of the best stagger distance.

The above studies were wind tunnel experiments based on varying the position of the canard with respect to the wing. In the present study the position of the wing was changed with respect to a canard placed in either a tandem or a staggered arrangement. This is because in aircraft the canard cannot be moved vertically owing to limitations of space. The primary objective was to determine the optimum position of the wing with respect to the canard, that is, the position where there were no trailing vortices of the canard affecting the flow conditions at leading edge of the wing. The experiments were carried out at low Mach numbers ($M < 0.2$).

Methodology and experimental setup

The Eagle 150 is a two-seater, single-engine, light aircraft. It is designed to be used as a trainer as well as a surveillance aircraft. It has a tandem wing design (canard at the front and wing behind it). The aircraft has a wing span of 7163 mm, chord 736.6 mm, aspect ratio 9.72. The canard span is 4879 mm, chord 736.6 mm, aspect ratio 6.4. The maximum speed is 240 km/h and stall speed (clean) is 101 km/h. The front view, plan view and side view of the aircraft are shown in Fig. 1.

The aerodynamic tests were carried out in an open-circuit wind tunnel (Fig. 2) at a speed of 38 m/s. The test section of the wind tunnel is 300 mm × 300 mm and 600 mm long.

The two airfoils were made from fibreglass, with semi-span aspect ratios for the canard of 6.4 and for the wing of 9.2. Wind tunnel tests were carried out for two separate cases. The airfoils were first tested isolated at 38 m/s to get the coefficient of lift at various angles of attack. A second series of experiments was then conducted for different tandem/staggered positions of the airfoils at the same wind tunnel speed and at 0° angle of attack. The wind tunnel test section with the canard and airfoil is shown in Fig. 3 and the canard/wing configuration is shown in Fig. 4. The turbulent flow over the airfoil was established by making boundary layer measurements with the help of a Pitot-Static tube and a special boundary layer probe. This enabled us to select a k-ε turbulence model in computational analysis.

CFD analysis and fluent

Computational fluid dynamics (CFD) is a valuable tool with which to validate the wind tunnel results. The wings can be simulated in two dimensions because it is

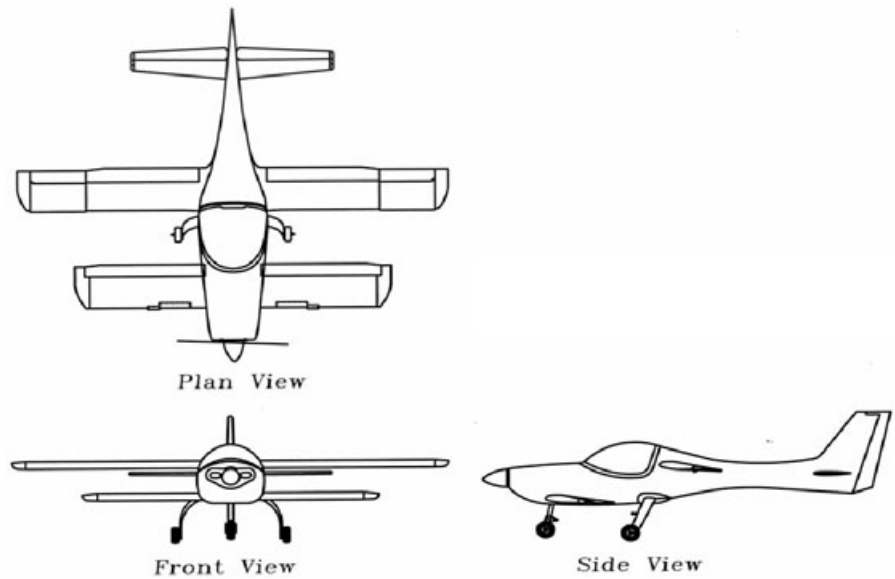

Fig. 1 *Front view, plan view and side view of the aircraft.*

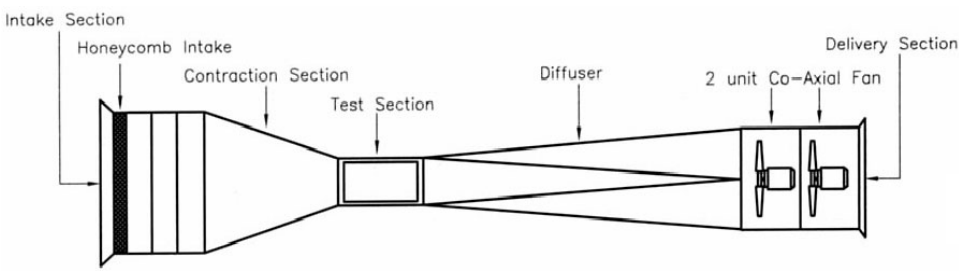

Fig. 2 *School of Mechanical Engineering, USM, open-circuit wind tunnel.*

assumed that the length of the wings is infinite and their cross-sectional area is constant throughout the length of the airfoil. For two-dimensional analysis of airfoils, numerical calculation methods based on potential theory are available. CFD code 5 has been used in the present analysis. The investigations were carried out with chord lengths of 92 mm for the canard and 62 mm for the wing. The models were meshed with GAMBIT using a pave-type unstructured mesh. GAMBIT is a software package designed to analyse, design and build mesh for CFD and other scientific applications. The angle of attack for both airfoils varied from 0° to 14°. For a single airfoil, the number of mesh faces was 36 432 and for the tandem wing configuration a total

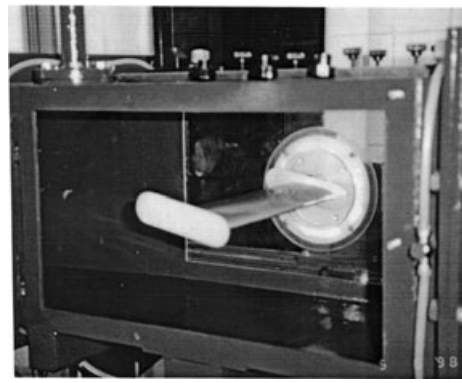

Fig. 3 *Wind tunnel section with canard airfoil.*

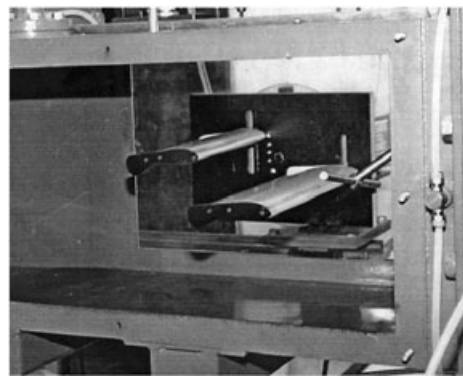

Fig. 4 *Canard/wing configuration model.*

of 31 322 mesh faces were generated, whereas for the staggered wing configuration ($z/c = 0.44$) the number of mesh faces was 31 382. The meshed airfoil models were then exported into FLUENT 5 to set the boundary conditions and to solve the equation. The simulation was carried out for the same conditions as the wind tunnel tests: air speed 38 m/s, turbulence intensity 2.5%, and ambient temperature of 300 K. The simulation results included lift and drag coefficients, velocity vector profile and pressure contour.

However, there is a certain amount of discrepancy between experimental measurements and CFD predictions. The turbulence intensity in the wind tunnel was not measured but in the CFD analysis it was taken as 2.5%. While doing CFD analysis, in the options available in the column for 'material', a factor for roughness was not

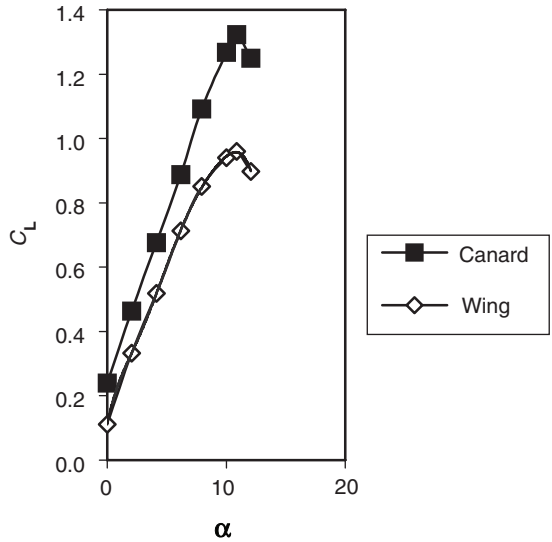

Fig. 5 *Lift coefficient vs angle of attack (wind tunnel experiment).*

included, whereas, in the real situation in the wind tunnel, there is certain amount of roughness on the airfoils. Again, in the CFD analysis model it was assumed that the flow over the aerofoil is fully turbulent, whereas initially the flow on the airfoil is laminar and later becomes turbulent and is fully turbulent at the trailing edge of the airfoils.

Results and discussion

Fig. 5 plots the coefficient of lift, C_L, as a function of angle of attack, α. The coefficient of lift varies with angle of attack and increases up to the stall angle for both the airfoils. The stall angle for both the airfoils is 11°. The maximum value of C_L for the canard was 1.32 and for the wing was 0.96.

Fig. 6 shows wind tunnel and computational results for both airfoils. The computational results coincide with the wind tunnel results at all angles of attack for the canard. However, there is a difference in the computational and experimental results for the wing airfoil. The deviation is almost constant at all values of angle of attack.

Fig. 7(a, b) plots the velocity profile of the boundary layer growth on the wing at distances $x = 15.5$ mm and $x = 62$ mm respectively along the chord from the leading edge. Similarly, Fig. 8(a, b) shows the velocity profile at distances $x = 29.5$ mm and $x = 88$ mm respectively along the chord for the canard from the leading edge. The velocity, V, is measured by Pitot-Static tube and is given by $V = (2\mathrm{d}p/\rho)^{1/2}$ where $\mathrm{d}p = p_0 - p$, the difference between total and static pressure, and ρ is the density of air. V_∞ refers to the upstream velocity in the test section.

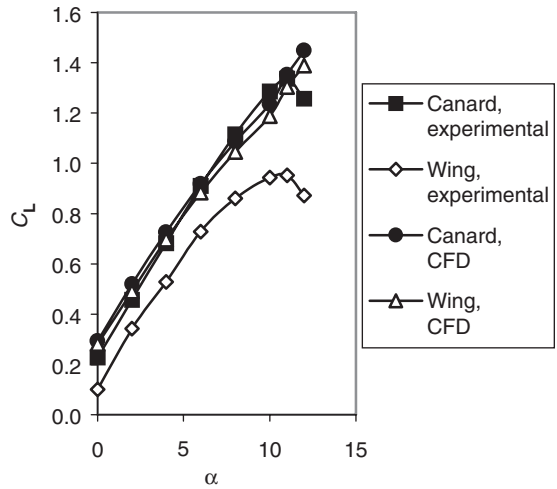

Fig. 6 *Lift coefficient vs angle of attack (CFD and wind tunnel).*

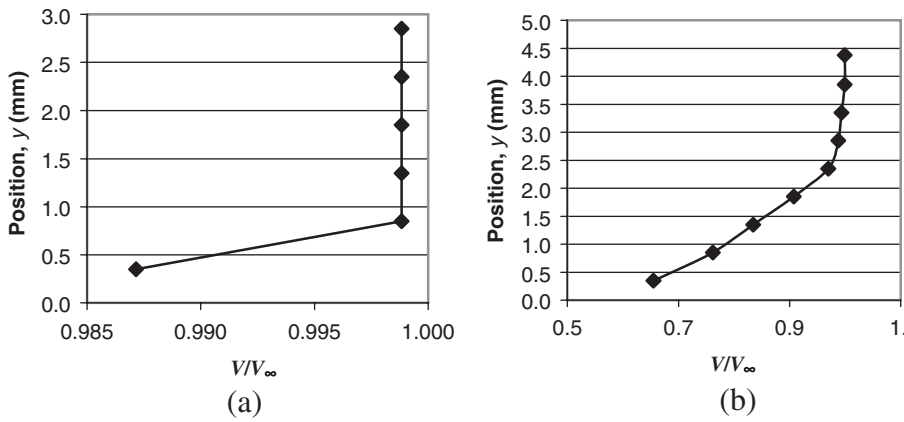

Fig. 7 *Velocity profile for the wing: (a)* x = *15.5 mm, (b)* x = *62 mm.*

From the fundamentals of fluid mechanics, laminar/turbulent thickness over a flat plate with zero pressure gradient depends on the Reynolds number and is given by the following equations:

$$\text{laminar flow:} \quad \delta/x = 5/(\mathrm{Re}_x)^{1/2}$$

$$\text{turbulent flow:} \quad \delta/x = 0.37/(\mathrm{Re}_x)^{1/5} \tag{1}$$

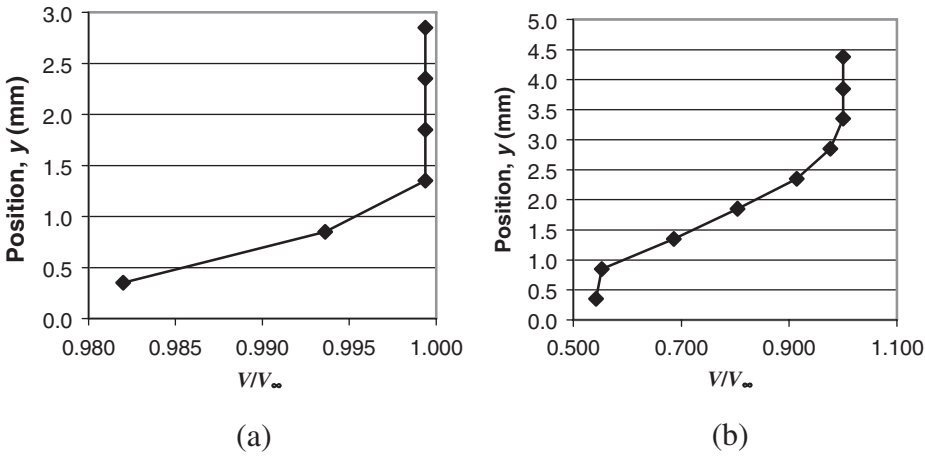

Fig. 8 *Velocity profile for the canard: (a)* x = *29.5 mm, (b)* x = *88 mm.*

where $\mathrm{Re}_x = \rho V x/\mu$, δ is the boundary layer thickness at that section of airfoil and x is the distance from the leading edge of the airfoil along the chord. However, the experiments were carried out on a curved surface (airfoil) with a pressure gradient and this might help to explain why the theoretical values and measured values did not match. The practical values of boundary layer thickness are higher than the theoretical values and therefore it is established that turbulent flow exists throughout and it is justified to use the k-ε turbulent model for simulation.

Fig. 9 shows the side view of the canard–wing configuration obtained by kinematic similarity between model and prototype. Fig. 10 indicates the tandem/staggered position of the airfoils; position 0–0 refers to $z/c = 0$, position 0–1 refers to $z/c = 0.22$, and position 0–2 refers to $z/c = 0.44$, where z refers to the vertical distance from the center of the airfoils and c is the chord of the airfoils. The stagger along the length of airfoils was kept constant. Fig. 11 shows the relation between the coefficient of lift, C_L, and the angle of attack, α, at various positions of the wing. The unfavorable lift coefficient for the low configuration (0–1) is evident as the angle of attack increases. The configuration has maximum lift coefficient at position 0–2, which is the optimum position of the wing with respect to the canard. There is also discontinuity between the angles of attack of 6° and 8°. The lift force reading of electronic balance could not be taken due to severe vibrations set up in the airfoils. The staggered positions exhibit stalls at two angles of attack, $\alpha = 4.8°$ and $\alpha = 11°$, compared with $\alpha = 9°$ for a tandem position.

Fig. 12(a, b) shows the velocity profile and pressure contour of the canard and wing, respectively; the two contours are practically the same for both the airfoils. Fig. 13(a, b) shows the velocity vector profile and pressure contour for the tandem

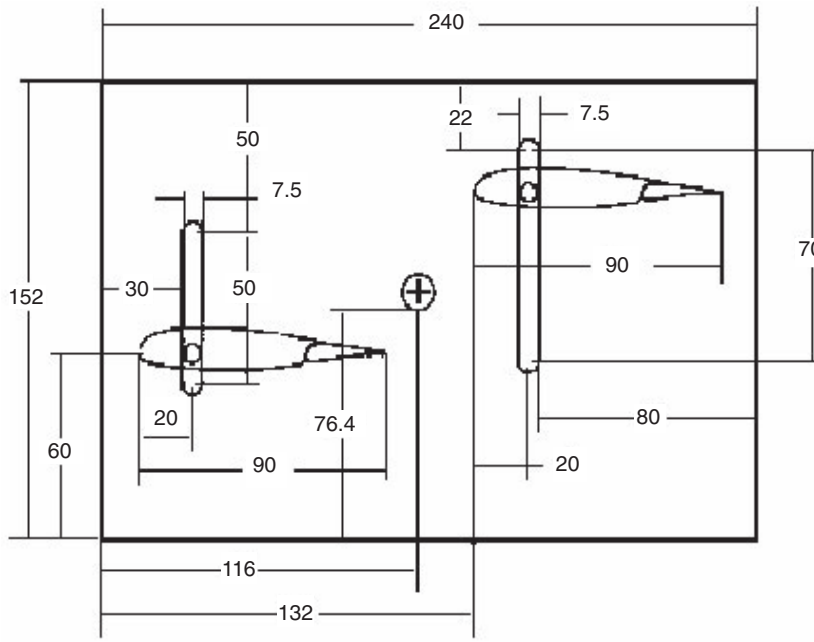

Fig. 9 *Canard–wing configuration. All dimensions are in mm.*

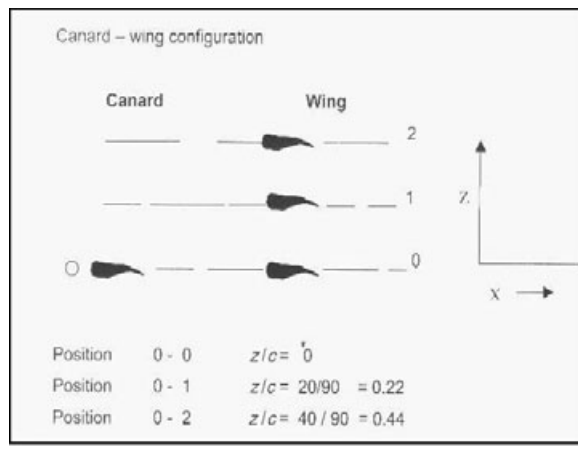

Fig. 10 *Canard–wing configuration: the three positions of the wing with respect to the canard.*

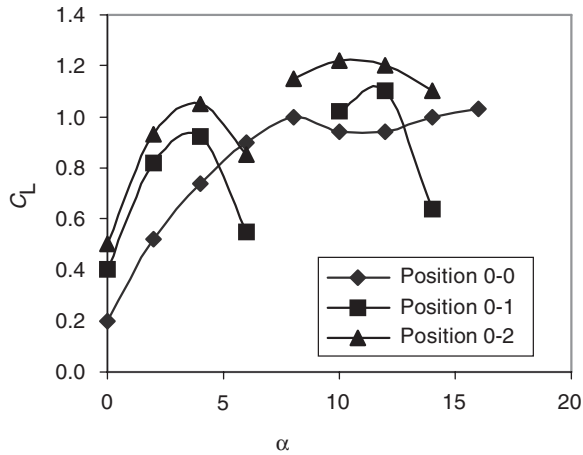

Fig. 11 *Plots of coefficient of lift and angle of attack at various positions of wings: 0–0, 0–1, 0–2.*

arrangement ($z/c = 0$). On comparing the velocity contour of the airfoil, one can see the wake produced by the leading airfoil extending up to the leading edge of the trailing airfoil and disturbing the flow at the inlet. Thus the velocity at the inlet for the trailing airfoil cannot be considered uniform.

Fig. 14(a, b) shows the velocity vector profile and pressure contour for the staggered arrangement ($z/c = 0.44$). It is shown that the wake produced by the leading airfoil does not disturb the flow of the trailing airfoil; however, the velocity vector passing over the canard is drifted upwards and disturbs the flow at inlet of the wing. The flow visualization tests conducted with a smoke generator in the wind tunnel for the wing/canard configurations at 0–0, 0–2 positions is shown in Fig. 15(a, b). The tests show clearly that, at position 0–0, airflow at exit from the canard disturbs the inlet flow of the wing.

Conclusions

The two-dimensional analysis of wing and canard using the k-ε turbulence model has shown excellent results, as validated by the wind tunnel results. The experimental and simulation results for C_L against angle of attack coincide. The wind tunnel experiments for the tandem/staggered positions of the airfoils have given the optimum position for the wing and have been validated by simulation. The simulation results also show that with the tandem position, the wake created by the leading airfoil disturbs the inflow at the trailing airfoil.

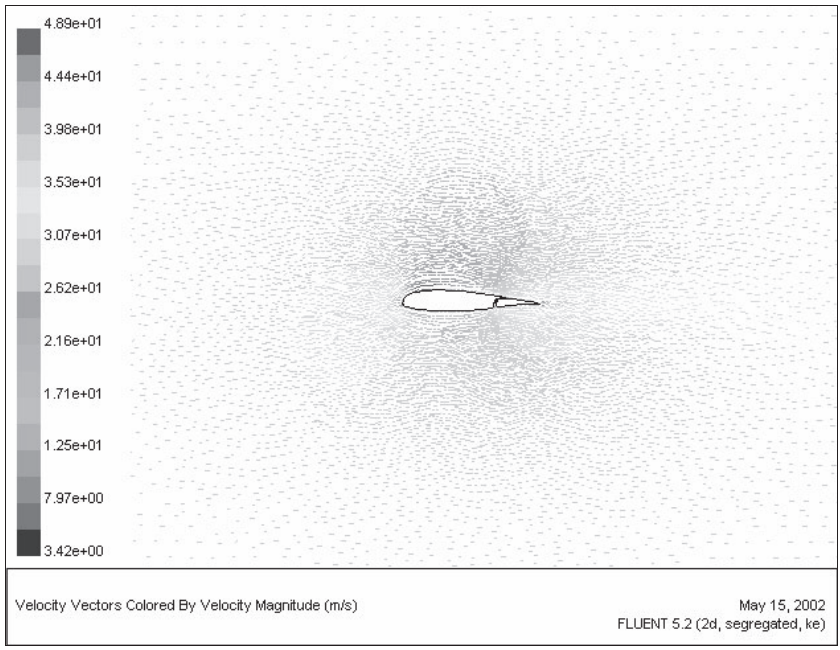

(a)

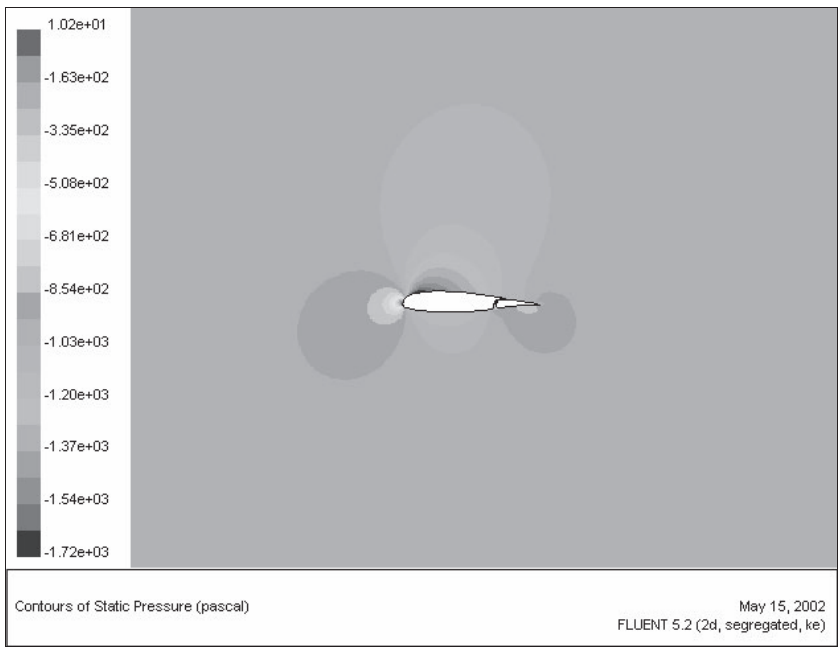

(b)

Fig. 12 *(a) Velocity vector of canard. (b) Pressure contour of canard.*

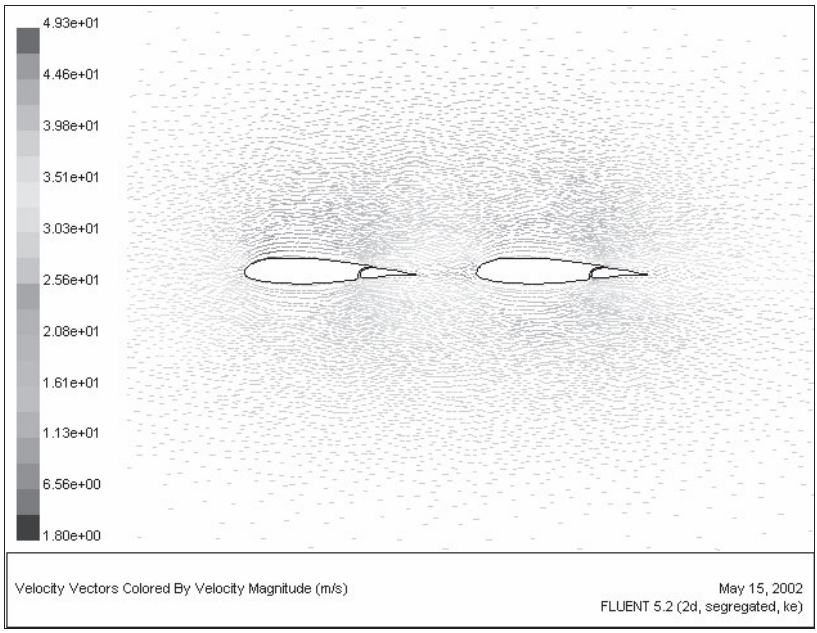

(a)

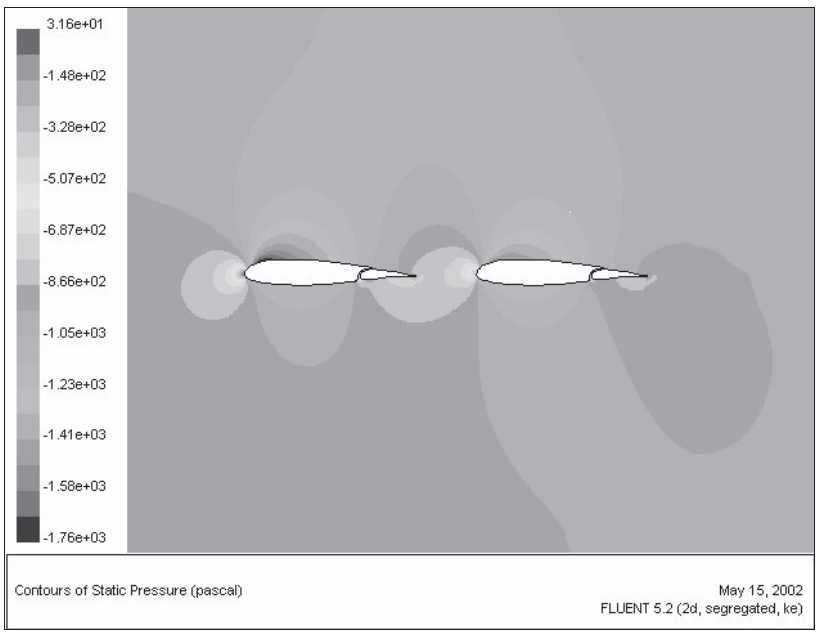

(b)

Fig. 13 *(a) Velocity vector of tandem arrangement, z/c = 0. (b) Pressure contour of tandem arrangement, z/c = 0.*

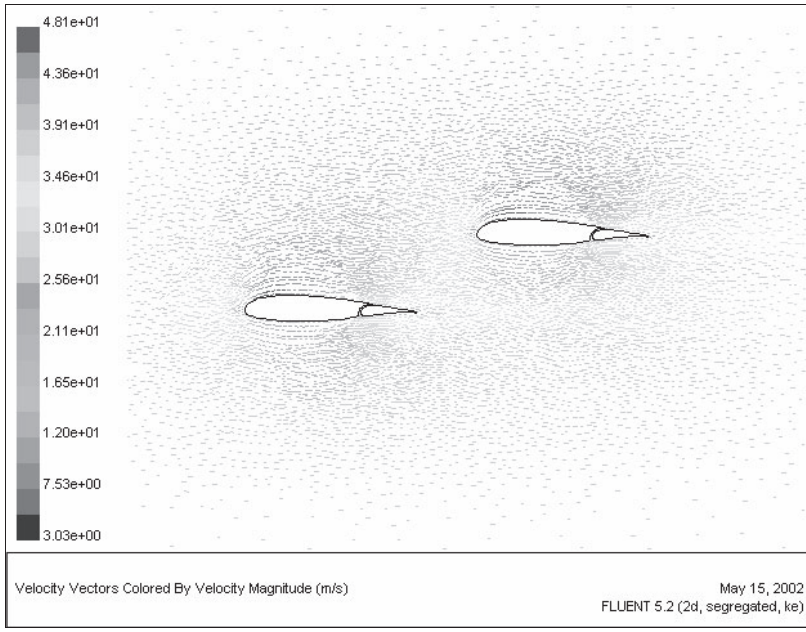

(a)

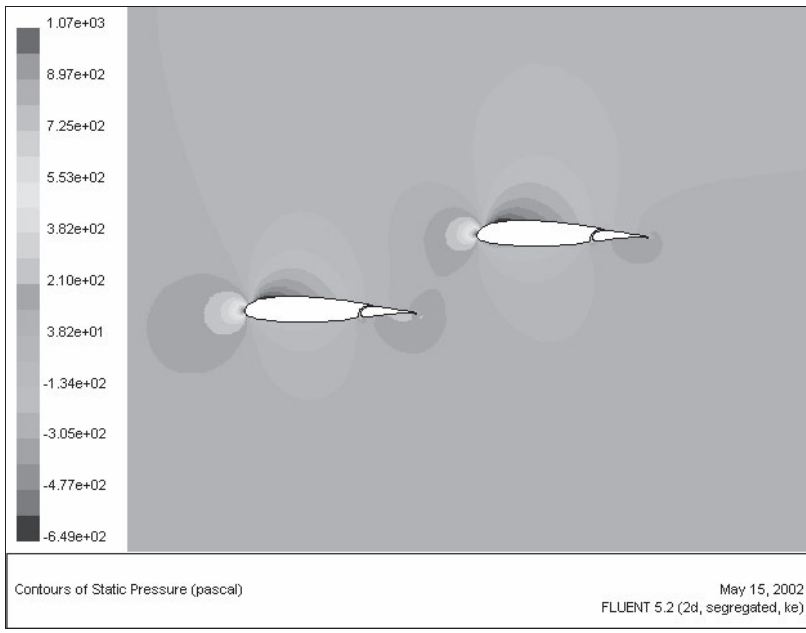

(b)

Fig. 14 *(a) Velocity vector of staggered arrangement, z/c = 0.44. (b) Pressure contour of staggered arrangement, z/c = 0.44.*

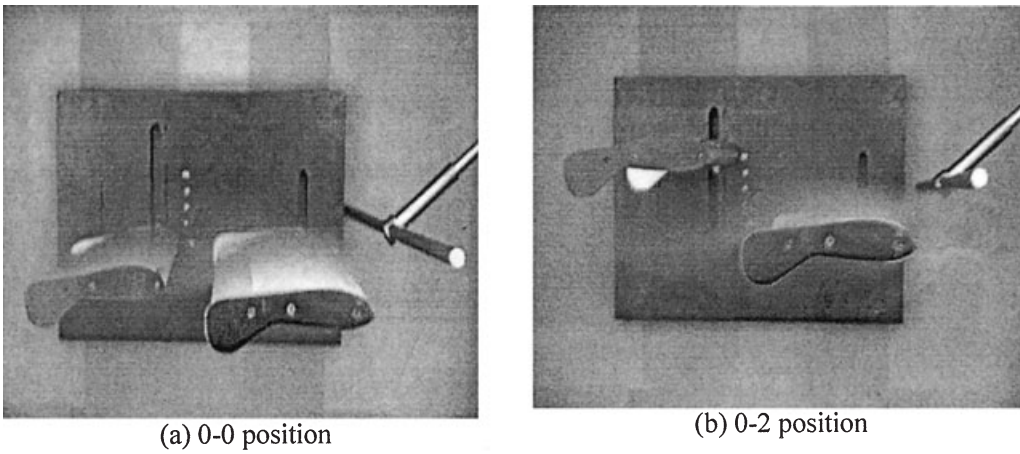

Fig. 15 *Flow visualization test: (a) 0–0 position; (b) 0–2 position.*

References

[1] T. McGree and I. Kroo, 'A fundamental comparison of canard and conventional configurations', *Journal of Aircraft*, **20**(11) (1983).
[2] W. Calarese, 'Closed coupled canard–wing vortex interaction', *Journal of Aircraft*, **21**(2) (1984).
[3] E. L. Tu, 'Effect of canard position on the longitudinal aerodynamic characteristics of a close-coupled canard–wing body configurations', *AIAA* (1992), 1–11.
[4] D. Fanjoy and D. J. Dorney, 'A study of tandem-airfoil interaction in different flight regimes', *AIAA* 97-0515 (1997).